Tandem catalysis for the production of alkyl lactates from ketohexoses at moderate temperatures

Marat Orazov and Mark E. Davis[1]

Chemical Engineering, California Institute of Technology, Pasadena, CA 91125

Contributed by Mark E. Davis, August 19, 2015 (sent for review August 1, 2015)

Retro-aldol reactions have been implicated as the limiting steps in catalytic routes to convert biomass-derived hexoses and pentoses into valuable C_2, C_3, and C_4 products such as glycolic acid, lactic acid, 2-hydroxy-3-butenoic acid, 2,4-dihydroxybutanoic acid, and alkyl esters thereof. Due to a lack of efficient retro-aldol catalysts, most previous investigations of catalytic pathways involving these reactions were conducted at high temperatures (≥160 °C). Here, we report moderate-temperature (around 100 °C) retro-aldol reactions of various hexoses in aqueous and alcoholic media with catalysts traditionally known for their capacity to catalyze 1,2-intramolecular carbon shift (1,2-CS) reactions of aldoses, i.e., various molybdenum oxide and molybdate species, nickel(II) diamine complexes, alkali-exchanged stannosilicate molecular sieves, and amorphous TiO_2–SiO_2 coprecipitates. Solid Lewis acid cocatalysts that are known to catalyze 1,2-intramolecular hydride shift (1,2-HS) reactions that enable the formation of α-hydroxy carboxylic acids from tetroses, trioses, and glycolaldehyde, but cannot readily catalyze retro-aldol reactions of hexoses and pentoses at these moderate temperatures, are shown to be compatible with the aforementioned retro-aldol catalysts. The combination of a distinct retro-aldol catalyst with a 1,2-HS catalyst enables lactic acid and alkyl lactate formation from ketohexoses at moderate temperatures (around 100 °C), with yields comparable to best-reported chemocatalytic examples at high temperature conditions (≥160 °C). The use of moderate temperatures enables numerous desirable features such as lower pressure and significantly less catalyst deactivation.

retro-aldol reactions | alkyl lactates | heterogeneous catalysis

Chemocatalytic routes for the production of α-hydroxy carboxylic acids, e.g., glycolic acid, lactic acid, 2-hydroxy-3-butenoic acid, and 2,4-dihydroxybutanoic acid, from biomass-derived sugars have been extensively investigated in the recent years, as these acids, as well as their esters and lactones, have been recognized to have a large potential to function as renewable, platform chemicals for a number of applications such as polymers, solvents, and fine chemicals (1–7). Considerable progress has been achieved with the production of lactic acid and alkyl lactates from trioses [glyceraldehyde (GLA) and dihydroxyacetone (DHA)], with nearly quantitative yields obtained with state-of-the-art catalysts, e.g., tin-containing zeotypes Sn-Beta and Sn-MFI, which are known for their capacity to catalyze 1,2-intramolecular hydride shift (1,2-HS) reactions, at moderate temperatures (around 100 °C) (8). Similarly, the C_2 and C_4 products (glycolic acid, 2-hydroxy-3-butenoic acid, 2,4-dihydroxybutanoic acid, and esters thereof) can be produced in good yields when glycolaldehyde, glyoxal, or tetroses (erythrose, threose, and erythrulose) are used as substrates (4, 6). However, the substrates required for these reactions are not easily obtained or isolated from biomass, as the majority of terrestrial biomass comprises cellulose and hemicellulose (polymers of hexoses and pentoses) (5).

To enable the formation of these C_2–C_4 α-hydroxy carboxylic acids from cellulosic and hemicellulosic biomass, retro-aldol reactions are required to fragment the hexose and pentose carbon backbones (r_2 and r_3 in Fig. 1). For the common aldoses and ketoses, these C–C bond-splitting reactions have large activation energies and unfavorable thermodynamics at low-to-moderate temperatures. As a result, most attempts at the catalytic production of C_2–C_4 α-hydroxy carboxylic acids from hexoses and pentoses have involved high temperatures (≥160 °C) (3, 9). Carbon basis yields of ∼64–68% of methyl lactate at full conversion were reported for reactions of sucrose catalyzed by Sn-Beta at 160 °C for 20 h (3). Lower yields of ∼40–44% were reported for monosaccharide substrates in the same study (3). Recently, methyl lactate yields upwards of 75% from sucrose were achieved with Sn-Beta at 170 °C, when specific amounts of alkali carbonates were added to the reaction system (9). Furthermore, the authors suggested that, in the initial study involving Sn-Beta, materials were possibly contaminated by alkali during synthesis, and that alkali-free Sn-Beta recently led to lower yields (30%) (9).

Low thermal stability of sugars at high temperatures and lack of substrate and reaction specificity of the catalytic sites investigated in the aforementioned systems likely lead to dehydration reactions of ketohexoses to 5-hydroxymethyl furfural (5-HMF) (r_5 in Fig. 1). The subsequent fragmentation and coupling reactions of 5-HMF can lead to the formation of insoluble humins that deposit on the catalyst, thereby leading to deactivation and loss of yield of useful products. Large-pore catalysts like Sn-Beta can promote aldose–ketose isomerization reactions (r_1 in Fig. 1) of substrates as large as disaccharides (10) because the Lewis acid sites that are active for 1,2-HS reactions are accessible to such species. The same Lewis acid sites have been previously proposed as the active sites in retro-aldol reactions (8). This inability of Sn-Beta (and other 12-MR materials) to perform size-dependent reaction discrimination results in aldose–ketose interconversion and parallel retro-aldol reactions of aldohexoses and ketohexoses. Thus, even when ketohexose substrates are used, C_2 and C_4 products derived from aldoses concomitantly form with the more desired C_3 products derived from ketoses (r_4 and r_7–r_{10} in Fig. 1, respectively) (3). Because of these features, catalytic strategies that allow for retro-aldol reactions of hexoses to proceed in the

Significance

Retro-aldol reactions of biomass-derived monosaccharides enable the production of a number of industrially relevant, renewable platform chemicals (e.g., C_2–C_4 α-hydroxy carboxylic acids, acrylic acid, and esters thereof; and ethylene and propylene glycol). Here, we show a set of retro-aldol catalysts that can perform these reactions at significantly lower temperatures (∼100 °C) than previously reported, and demonstrate that these catalysts enable the key retro-aldol step when used in combination with a 1,2-hydride shift catalyst to create a reaction cascade that converts ketohexoses to lactic acid. The use of moderate temperatures enables numerous desirable features such as lower pressure and significantly less catalyst deactivation.

Author contributions: M.O. and M.E.D. designed research; M.O. performed research; M.O. and M.E.D. analyzed data; and M.O. and M.E.D. wrote the paper.

The authors declare no conflict of interest.

Freely available online through the PNAS open access option.

[1]To whom correspondence should be addressed. Email: mdavis@cheme.caltech.edu.

This article contains supporting information online at www.pnas.org/lookup/suppl/doi:10.1073/pnas.1516466112/-/DCSupplemental.

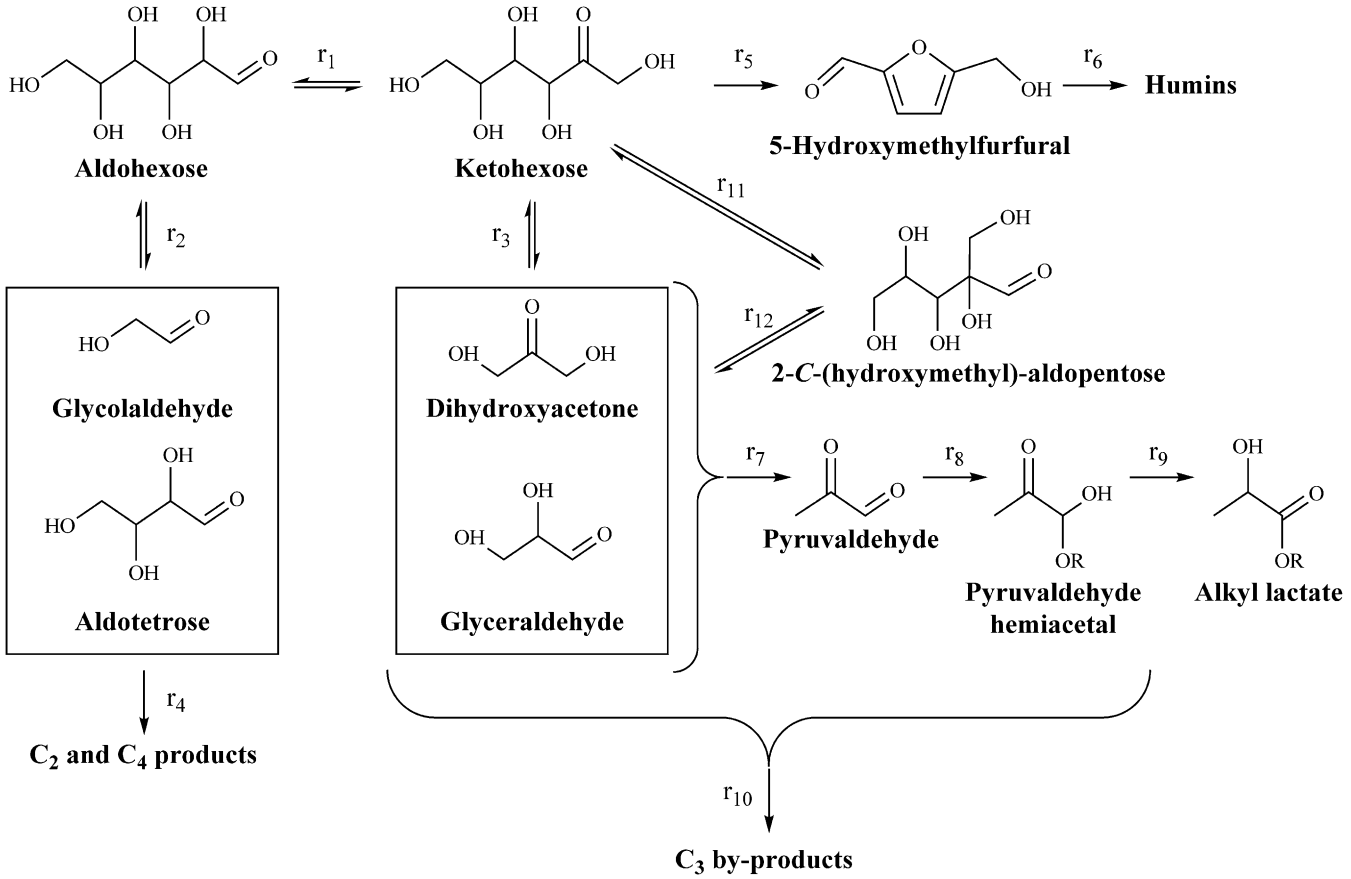

Fig. 1. Schematic representation of reaction network in which ketohexoses can isomerize to aldohexoses via 1,2-HS (r_1) and to 2-*C*-(hydroxymethyl)-aldopentoses via 1,2-CS (r_{11}) reactions. Retro-aldol reactions of hexose species (r_2, r_3, and r_{12}) lead to the formation of C_2, C_3, and C_4 carbohydrate fragments. Lewis acids can then catalyze the formation of α-hydroxy carboxylic acids from these smaller fragments (e.g., r_7, r_8, and r_9 in the formation of alkyl lactate from trioses). Side reactions, involving dehydration reactions of fructose to 5-HMF (r_5), redox and fragmentation reactions of unstable intermediates, and various humin-forming condensation reactions, lead to loss of yield of desired products.

absence of aldose–ketose isomerization would be highly useful, as they would have the potential to significantly affect the distribution of C_2, C_3, and C_4 products.

Here, we report moderate-temperature (around 100 °C) retro-aldol reactions of various hexoses in aqueous and alcoholic media with catalysts traditionally known for their capacity to catalyze 1,2-intramolecular carbon shift (1,2-CS) reactions of aldoses, i.e., various molybdenum oxide and molybdate species, nickel(II) diamine complexes, alkali-exchanged stannosilicate molecular sieves, and amorphous TiO_2–SiO_2 coprecipitates. Because these catalysts do not readily catalyze aldose–ketose interconversion through 1,2-HS, they are candidate cocatalysts for reaction pathways that benefit from aldose- or ketose-specific, retro-aldol fragmentation. Here, these retro-aldol catalysts are combined with solid Lewis acid catalysts to enable the moderate-temperature conversion of hexoses into α-hydroxy carboxylic acids.

Results and Discussion

Retro-Aldol Reactions and 1,2-CS Catalysts. During our recent investigation of epimerization reactions of aldohexoses on alkali-exchanged Sn-Beta materials, a change in the reaction pathway from a 1,2-HS to a 1,2-CS upon alkali exchange was observed (11). This 1,2-CS pathway in aldohexoses is analogous to those previously reported for molybdate- and nickel(II) diamine-catalyzed reactions of these aldoses (also known as Bilik reaction), where simultaneous C–C bond-breaking and -forming steps were proposed to occur (*SI Appendix*, Scheme S1) (12, 13). Reactions of ketoses catalyzed by molybdates and nickel(II) diamines were found to proceed through analogous pathways to form branched sugars [2-*C*-(hydroxymethyl)-aldoses] (r_{11} in Fig. 1) (14–16). In addition to the branched sugars, small amounts of ketose isomers were observed, e.g., when D-fructose was reacted with molybdate, the branched sugar D-hamamelose formed, as well as small quantities of ketose isomers: sorbose, psicose, and tagatose (14, 17). The formation of ketose isomers was attributed to competing hydride shift side reactions (17).

Like with molybdates, we observed the formation of the same branched sugar (D-hamamelose) and ketose isomers when fructose was reacted with alkali-exchanged Sn-Beta at 100 °C. Interestingly, small quantities of the retro-aldol products, DHA and GLA, were also observed in the high-performance liquid chromatography (HPLC) chromatograms and nuclear magnetic resonance (NMR) spectra of unseparated reaction solutions. The presence of DHA and GLA raises questions about the mechanism of ketose isomer formation, as it is possible to form all of the ketohexoses through nonstereospecific aldol condensation of DHA and racemic GLA. When water-dissolved MoO_3 (H_2MoO_4) was tested as a catalyst with fructose as substrate (reacted at 100 °C), initial formation of hamamelose, DHA, and GLA was observed. Subsequently, sorbose, tagatose, and psicose appeared, without significant changes in the DHA and GLA concentration. Quantification of products was not performed due to a multitude of partially overlapping peaks in HPLC chromatograms and NMR spectra. However, fructose and sorbose were eventually observed in substantially greater quantities than tagatose, psicose, and hamamelose. Fractionation of product solutions and ^1H and ^{13}C NMR were used to confirm the presence

of DHA, GLA, fructose, sorbose, tagatose, psicose, and 2-*C*-(hydroxymethyl)-aldopentoses (*SI Appendix*, Figs. S1–S6). These results suggest that some of the ketose isomers may form as aldol condensation products of DHA and GLA, rather than directly from fructose through hydride shift reactions, as was previously hypothesized. The unfavorable equilibria of retro-aldol reactions at these moderate temperatures may be responsible for the low concentrations of DHA and GLA. The reverse reaction, aldol coupling, is a logical secondary reaction that can form the more stable ketohexose side products. The possibility of aldol coupling was confirmed by reacting a mixture of DHA and GLA under the same conditions, resulting in complex mixture of products containing ketohexoses and 2-*C*-(hydroxymethyl)-aldopentoses.

Although the low production of 2-*C*-(hydroxymethyl)-aldopentoses may be due to thermodynamic limitations, e.g., hamamelose–fructose equilibrium K_{eq} ~14 (14), tagatose and psicose may form in small quantities due to kinetic reasons. The tetradentate open-chain ketohydrol fructose–molybdate complex that was previously hypothesized to be the key species in the fructose–hamamelose rearrangement catalyzed by water-dissolved molybdates is shown in *SI Appendix*, Scheme S2 (along with analogs for other ketohexoses) (14). ^{1}H and ^{13}C NMR studies of the molybdate complexes of ketohexoses suggest that only fructose and sorbose form detectable amounts of tetradentate molybdate complexes, whereas psicose and tagatose tend to form tridentate complexes (18). These results suggest that aldol coupling reactions that would lead to the formation of tagatose and psicose would proceed through more energetic transition states, with slow kinetics. Furthermore, psicose and tagatose complexes appear more stable, with 80–95% of the sugars bound to Mo (at stoichiometric Mo/monosaccharide amounts), whereas these values for sorbose and fructose are only 15–20% (18). If the retro-aldol reactions of ketohexoses proceed through tetradentate molybdate complexes, these results suggest that the formation of tagatose and psicose may reduce the fraction of catalytically active molybdate species through competitive binding and formation of tridentate complexes.

Although binuclear molybdate species were implicated in epimerization reactions catalyzed by water-dissolved MoO_3, higher structures containing molybdate ions were later shown to also catalyze epimerization reactions, e.g., Keggin structure molybdenum-based polyoxometalates (19), and heptamolybdate species immobilized on anion exchange supports (20). Similarly, we observe the promotion of retro-aldol reactions of fructose by the $H_3PMo_{12}O_{40}$ Keggin ion, and by $(NH_4)_6Mo_7O_{24}$, both as homogeneous catalysts and when immobilized onto an anion exchange support, e.g., Amberlite IRA-400, chloride form. Soluble and insoluble molybdate salts, e.g., Na_2Mo_4 and $ZnMoO_4$, respectively, as well as insoluble solids containing Mo(IV), e.g., MoO_2, and MoS_2, also are catalytically active in retro-aldol reactions of fructose in our hands. At this time, it is not clear whether the nominal form of each starting compound is the catalytically active one, or whether unknown catalytic species are generated in situ at reaction conditions. Due to the aforementioned complications in quantification, we could not directly assess the performance of each catalyst in retro-aldol reactions. However, we did observe differences in kinetics (see below) of the lactate-forming reaction cascade when different Mo-containing species were used for the retro-aldol component of the pathway, i.e., r_3 of cascade consisting of r_3, and r_7–r_9 in Fig. 1.

Tungstate analogs of molybdate-monosaccharide complexes have been reported to have formation constants that are 2–3 orders of magnitude higher than molybdates (21). Such strong binding may be responsible for the apparent lack of catalytic activity of H_2WO_4 and $H_3PW_{12}O_{40}$ in the epimerization of glucose to mannose at mild conditions (19, 22). Similarly, in our experiments, tungstate species performed poorly but did produce species consistent with retro-aldol reactions of hexoses at long reaction times. Interestingly, at high temperatures (≥150 °C), H_xWO_3 was recently reported to catalyze retro-aldol reactions of glucose and fructose, when coupled with a Ru/C-promoted H_2-reductive step to produce glycols (23). An apparent activation energy of 141.3 kJ/mol for the retro-aldol reaction of glucose was reported, whereas the apparent activation energy for further reactions of glycolaldehyde (including aldol condensation) was estimated to be 52.7 kJ/mol (23). These results illustrate the high barriers of retro-aldol reactions.

Nickel(II) diamine complexes in methanolic solutions were previously shown to catalyze the 1,2-CS in aldoses (13) and 2-*C*-(hydroxymethyl)-aldopentose formation from ketohexoses (16) at temperatures around 60 °C. We observed that $[Ni(N,N,N',N'\text{-}Me_4en)_2]Cl_2$ in methanol also accelerated the retro-aldol part of the methyl lactate-producing reaction cascade at temperatures around 100 °C.

Coupling Retro-Aldol Reactions with 1,2-HS for Lactate Production. Materials that can catalyze the 1,2-CS in aldoses were reported to be poor 1,2-HS catalysts for the same substrates, as the production of ketoses was not detected (17). Because the formation of lactate from trioses by Lewis acid catalysts has been shown to involve a 1,2-HS (r_9 in Fig. 1) (24), an efficient route to the more thermodynamically stable lactate products is not enabled by the retro-aldol catalysts described above (resulting in triose accumulation and recombination through aldol reactions). Addition of a 1,2-HS cocatalyst [Sn-MFI with Si/Sn = 70 ± 6, fluoride-free synthesis (25)] to a 1 wt% fructose, 0.2 wt% MoO_3 aqueous solution enabled formation of lactic acid at 100 °C. However, ^{1}H NMR data suggest that the lactate formed strong pH-dependent complexes with molybdate species (*SI Appendix*, Fig. S7), and that lactate production stopped once the stoichiometric amount of 2 mol of lactate per mole of molybdate was produced. This inhibition of catalysis by product coordination is consistent with the previously reported pH-dependent molybdate–lactate complex formation, with an estimated pK of formation of −49 at pH = 4.5 (26).

When the reactions of fructose with MoO_3 and Sn-MFI were performed in alcoholic media, corresponding alkyl lactates were produced in good yields (see Fig. 2 for a representative graph of ethyl lactate production from fructose as a function of time at different temperatures, *SI Appendix*, Fig. S8, for ^{1}H NMR of methyl lactate product, and Table 1 for the maximum observed yields of lactate products under various reaction conditions). Turnover numbers (TONs) in excess of unity indicate that alkyl

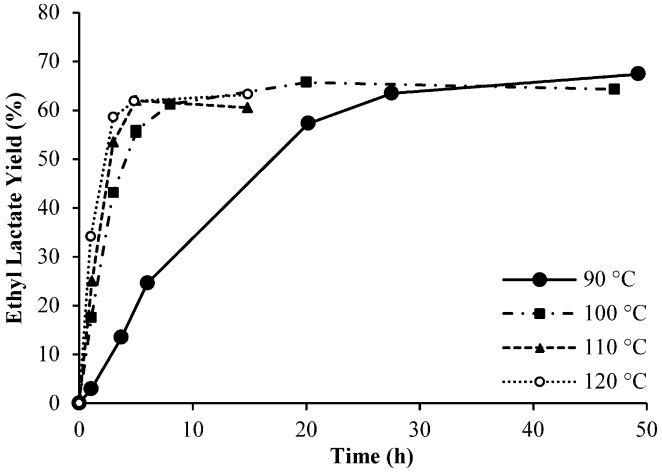

Fig. 2. Ethyl lactate yield as a function of time at different temperatures (indicated in legend). Reaction conditions were as follows: 80 mg of MoO_3, 100 mg of Sn-MFI, 50 mg of D-fructose, 4.9 g of EtOH, and 50 mg of naphthalene as internal standard.

Table 1. Maximum observed yields of lactic acid or alkyl lactates obtained under various reaction conditions

Reaction	1,2-CS catalyst, mass/mg		1,2-HS catalyst, mass/mg		Substrate, wt%		Solvent	Temperature, °C	Maximum yield, carbon basis, %
1	MoO_3	80	Sn-MFI	100	Fructose	1	EtOH	90	67.4
2	MoO_3	80	Sn-MFI	100	Fructose	1	EtOH	100	65.7
3	MoO_3	80	Sn-MFI	100	Fructose	1	EtOH	110	61.9
4	MoO_3	80	Sn-MFI	100	Fructose	1	EtOH	120	63.2
5	MoO_3	20	Sn-MFI	100	Fructose	1	EtOH	100	67.7
6	MoO_3	5	Sn-MFI	100	Fructose	1	EtOH	100	69.2
7	MoO_3	80	Sn-MFI	200	Fructose	1	EtOH	100	68.6
8	MoO_3	80	Sn-MFI	50	Fructose	1	EtOH	100	46.7
9	MoO_3	80	Sn-MFI	100	Fructose	5	EtOH	100	21.0
10	MoO_3	80	Sn-MFI	100	Fructose	0.2	EtOH	100	74.6
11		0	Sn-MFI	100	Fructose	1	EtOH	100	3.9
12		0	Sn-MFI	100	DHA/GLA	0.5/0.5	EtOH	100	86.5
13	MoO_3	80		0	Fructose	1	EtOH	100	13.0
14	MoO_3	80		0	DHA/GLA	0.5/0.5	EtOH	100	14.6
15	MoO_2	80	Sn-MFI	100	Fructose	1	EtOH	100	58.1
16	MoS_2	80	Sn-MFI	100	Fructose	1	EtOH	100	48.3
17	$H_3PMo_{12}O_{40}$	10	Sn-MFI	100	Fructose	1	EtOH	100	51.6
18	$Ni(Me_4en)_2Cl_2$	2	Sn-MFI	100	Fructose	1	MeOH	100	17.6*
19	$Ni(Me_4en)_2Cl_2$	20	Sn-MFI	100	Fructose	1	MeOH	100	45.1*
20	TiO_2-SiO_2	200	Sn-MFI	100	Fructose	1	MeOH	100	7.7
21	MoO_3	80	Sn-Beta	50	Fructose	1	EtOH	100	51.0
22	MoO_3	80	Sn-Beta	50	Glucose	1	EtOH	100	40.2
23		0	Sn-Beta	50	DHA	1	EtOH	100	88.4
24	MoO_3	80	Sn-MFI	100	Hamamelose	1	EtOH	100	70.2
25	MoO_3	80	Sn-MFI	100	Sorbose	1	EtOH	100	67.6
26	MoO_3	80	Sn-MFI	100	Psicose	1	EtOH	100	57.6
27	MoO_3	80	Sn-MFI	100	Tagatose	1	EtOH	100	46.1
28	MoO_3	80	Sn-MFI	100	Fructose	1	MeOH	100	68.2
29	MoO_3	80	Sn-MFI	100	Fructose	1	90 wt% EtOH 10 wt% H_2O	100	22.7
30	MoO_3	10	Sn-MFI	100	Fructose	1	H_2O	100	26.7†

Reactions were performed in 10-mL thick-walled crimp-sealed glass reactors that were heated in a temperature-controlled oil bath. Aliquots (~100 μL) were extracted and filtered with a 0.2-μm polytetrafluoroethylene syringe filter before analysis. Reaction conditions: for each reaction, the catalyst amounts, substrate concentrations, solvents, and temperature used are indicated in the table. Each reaction involving alcoholic solvents was performed with 4.9 g of solvent and 50 mg of naphthalene as internal standard for GC-FID quantification.

*For reactions with $[Ni(N,N,N',N'\text{-}Me_4en)_2]Cl_2$, aliquots were agitated with 20 mg of Dowex 50WX2 (hydrogen form) resin to remove nickel(II) species before filtration.

†For the reaction performed in water, no naphthalene was added, and 4,4-dimethyl-4-silapentane-1-sulfonic acid, sodium salt (DSS) was used as an external standard for quantitative ^{1}H-NMR.

lactate production is truly catalytic in such reactions, e.g., for reaction 6 in Table 1, the TON ≥ 5.5 based on Mo atoms for the retro-aldol reaction of fructose, and TON ≥ 16.1 based on Sn atoms for lactate formation from the resulting trioses. For reactions performed in alcoholic media, MoO_3 particles remained undissolved and progressively turned a dark-blue color, suggesting the possibility of partial reduction of MoO_3 or coverage with alcohol-insoluble molybdate–lactate complexes. Both possibilities could contribute to lowering of lactate yield. Rapid, reversible ketalization of ketoses by the solvent was observed and may influence the apparent reaction kinetics.

We investigated a number of parameters to maximize the yield of alkyl lactate products and gain further insight into the limiting factors of this reaction network. Time-dependent reaction profiles like those shown in Fig. 2 for the reactions accomplished and described in the following discussion are in *SI Appendix*, Figs. S9–S18. Data in Fig. 2 (reactions 1–4 in Table 1) show that, at otherwise-fixed conditions, increase in temperature resulted in an increased rate of ethyl lactate formation. Ultimately, ethyl lactate yield was not significantly impacted, suggesting that side reactions may have comparable activation energies to the limiting steps in lactate production. At 100 °C, with constant Sn-MFI amount, increasing the amount of MoO_3 catalyst led to a faster approach to the maximum lactate yield, but the increase in rate was not proportional to the change in MoO_3 amount (reactions 2, 5, and 6 in Table 1, and *SI Appendix*, Fig. S9). Additionally, a potential induction time is observed for the reaction with the lowest MoO_3 content. Conversely, fixing the amount of MoO_3, and varying the amount of Sn-MFI suggested that two regimes are possible: one where the ethyl lactate production is limited by retro-aldol reactions, i.e., excess Sn-MFI catalyst can deplete trioses faster than they are generated, and the other where the ethyl lactate production from trioses is kinetically relevant, i.e., insufficient Sn-MFI leads to accumulation of trioses (reactions 2, 7, and 8 in Table 1, and *SI Appendix*, Fig. S10). In the former scenario, the ultimate yield of ethyl lactate is higher than in the latter. Similarly, at fixed amounts of both catalysts, lower initial substrate concentrations result in higher ethyl lactate yields (reactions 2, 9, and 10 in Table 1, and *SI Appendix*, Fig. S11). These data suggest that high concentrations of substrate and intermediates are conducive to side-product formation and that rapid conversion to stable alkyl lactate products can reduce the extent of irreversible side reactions.

A set of control experiments that illustrate the importance of the combination of the two catalysts were performed (reactions 2 and 11–14 in Table 1, and *SI Appendix*, Fig. S12). In the absence of MoO_3 cocatalyst, Sn-MFI is unable to convert fructose to

ethyl lactate in significant yields, even though high yields of ethyl lactate are rapidly achieved by Sn-MFI alone when an equimolar mixture of DHA and GLA are used as substrates. Conversely, without Sn-MFI, MoO_3 slowly catalyzes the formation of ethyl lactate from fructose, with an ultimate ethyl lactate yield being considerably lower than in the mixed-catalyst system. Additionally, the use of equimolar DHA and GLA mixture as starting substrate does not result in significantly higher yields of ethyl lactate when MoO_3 is used by itself, further illustrating the rapidity of side reactions of trioses when a catalytic path to the thermodynamically stable lactate products is not present.

As discussed above, other Mo-containing 1,2-CS catalysts, e.g., MoO_2, MoS_2, $H_3PMo_{12}O_{40}$, Na_2MoO_4, $(NH_4)_6Mo_7O_{24}{\cdot}4H_2O$, $ZnMoO_4$, and $CaMoO_4$, were also able to accelerate alkyl lactate production from fructose when paired with Sn-MFI (reactions 15–17 in Table 1, and *SI Appendix*, Fig. S13, for the first three). Although the conditions for these catalysts have not been optimized, all alternative Mo-containing catalysts resulted in lower ethyl lactate yields than were achieved with MoO_3. Similarly, $[Ni(N,N,N',N'\text{-}Me_4en)_2]Cl_2$ in methanol also accelerated the retro-aldol part of the reaction cascade at 100 °C (reactions 18 and 19 in Table 1, and *SI Appendix*, Fig. S14), but deactivated after a few turnovers, in agreement with deactivation observed for aldose epimerization for similar complexes (13). This deactivation is potentially related to the formation of a white precipitate that was observed when $[Ni(N,N,N',N'\text{-}Me_4en)_2]Cl_2$ dissolved in MeOH was allowed to stand at ambient temperatures for extended times. Although nickel(II) diamines do not appear to be stable catalysts at reaction conditions, they are exceptionally active 1,2-CS catalysts (with 1,2-CS reactions of aldoses observed as low as 25 °C), and may be good model systems for retro-aldol reactions catalyzed by 1,2-CS catalysts, as their sugar complexes are isolable and amenable to characterization through extended X-ray absorption fine structure (EXAFS) analysis and X-ray crystallography (13). Amorphous TiO_2–SiO_2 coprecipitates were reported to slowly catalyze the 1,2-CS of glucose in methanol (10). Here, we observed only a minor increase in lactate production upon addition of TiO_2–SiO_2 coprecipitate to Sn-MFI (reaction 20 in Table 1, and *SI Appendix*, Fig. S14), and its use was not further investigated.

Sn-Beta [Si/Sn = 95 ± 14, fluoride synthesis (27)] can be used in place of Sn-MFI for the second part of the reaction cascade (reactions 21–23 in Table 1, and *SI Appendix*, Fig. S15). Furthermore, when coupled with MoO_3, under conditions where lactate formation from trioses was kinetically relevant, Sn-Beta performed better than Sn-MFI. This result is consistent with the reported faster kinetics of alkyl lactate synthesis from trioses by Sn-Beta than Sn-MFI (8). Because Sn-Beta can also catalyze glucose–fructose–mannose isomerization reactions through the 1,2-HS and, to some degree, retro-aldol reactions of hexoses, Sn-Beta was not used as the catalyst of choice in the current study, to avoid additional complicating factors in the reaction network. To illustrate this point, data in *SI Appendix*, Fig. S15, corresponding to reaction 22 in Table 1, show ethyl lactate formation from glucose when Sn-Beta is used in combination with MoO_3, thus indicating that aldose–ketose isomerization reactions occur on kinetically relevant timescales. Another noted benefit of using Sn-MFI as the 1,2-HS catalyst is that it can be easily synthesized in the absence of fluoride (25) (a frequently raised concern for large-scale syntheses of catalysts to be used for biomass processing, e.g., Sn-Beta). In principle, even more economically accessible materials that can catalyze lactate formation from trioses, e.g., postsynthetically treated Al zeolites (28) or homogeneous Lewis acids (29), may be paired with the retro-aldol catalysts reported in this study to produce alkyl lactates from hexoses at mild conditions.

Sn-Beta (and other Lewis acid-containing zeotypes, e.g., Ti-Beta) has also been shown to catalyze the 1,2-CS reactions of aldoses in aqueous solutions when either borate (30) or alkali salts (11) are present. The recently reported increase in methyl lactate production by Sn-Beta from fructose in methanol at 170 °C (from 16% to 57%) upon alkali carbonate addition (9) is consistent with formation of 1,2-CS sites upon alkali exchange of open sites in Sn-Beta. Sn-Beta systems with added borate and alkali salts were reported to be pH sensitive and are not efficient 1,2-CS catalysts in acidic conditions (11, 30). Furthermore, if Sn-MFI is used as a size-dependent 1,2-HS catalyst in conjunction with borate- or alkali-modified Sn-Beta, borate or alkali ions have the capacity to enter the Sn-MFI pores and influence the efficiency of lactate production from trioses. Thus, coupling of lactic acid or alkyl lactate production with retro-aldol reactions in mixed Sn-based zeotype systems was not studied here, but may warrant further investigation for the potential to affect the distribution of C_2, C_3, and C_4 products by limitation of aldose–ketose interconversion.

Formation of other 2-ketohexoses and 2-*C*-(hydroxymethyl)-aldopentoses in MoO_3-catalyzed reactions of fructose is discussed above. The differences in interactions between the various molybdate and hexose species may impact the rate of retro-aldol reactions. To test for this possibility, psicose, sorbose, tagatose, and hamamelose were reacted under the same conditions as fructose (reactions 2 and 24–27 in Table 1, and *SI Appendix*, Fig. S16). The rate of ethyl lactate formation from hamamelose is nearly identical to that from fructose. The initial rates of ethyl lactate formation from sorbose and psicose are lower than from fructose, but comparable ultimate yields of ethyl lactate are observed. Tagatose appears to be the slowest to react. Although it is clear that formation of ketohexose side products can impact the ultimate kinetics of ethyl lactate production, it is not certain whether the difference in the rates of retro-aldol reactions among these substrates is due to differences in energy barriers or due to reduction of available catalytic sites through competitive coordination in binding configurations that are not activated for retro-aldol reactions.

At 160 °C, Sn-Beta was reported to perform much better for lactate production from sucrose in methanol than in ethanol, isopropanol, or water (3). Here, for the case of MoO_3/Sn-MFI, no significant differences in kinetics or ultimate yields of alkyl lactates are observed between methanol and ethanol solvents, at 100 °C (reactions 2 and 28 in Table 1, and *SI Appendix*, Fig. S17). However, when 10 wt% water/90 wt% ethanol is used, the ultimate yield of ethyl lactate is significantly lower than for neat ethanol solvent (reactions 2 and 29 in Table 1, and *SI Appendix*, Fig. S17). This difference may be attributed to increased solubility of molybdate species in the mixed-solvent system. Because lactic acid forms strong complexes with molybdate ions, this fraction of lactate species is missing from the reported yield. In addition to the main alkyl lactate products quantified in this study, species consistent with retro-aldol reactions on aldohexoses and partially oxidized products were identified in the gas chromatography (GC)–mass spectrometry (MS) chromatograms of reaction solutions, e.g., ethyl acetals and ethyl esters of glycolaldehyde, glycolic acid, pyruvic acid, 2-hydroxy-3-butenoic acid, and 2,4-dihydroxybutanoic acid were observed for reactions in ethanol. Catalyst combinations that did not rapidly convert ketoses into alkyl lactates and generated Brønsted acidity also resulted in minor formation of 5-HMF and its partially oxidized variants, e.g., aqueous reactions of $H_3PMo_{12}O_{40}$ and Sn-MFI or H_2MoO_4 and Sn-MFI, after complete inhibitive complexation of lactic acid with molybdate. The aldohexoses that are required for C_2 and C_4 products are possibly formed in small amounts from ketohexoses by Sn sites on the external surface of Sn-MFI crystallites. We are currently evaluating retro-aldol reactions of aldoses for selective formation of C_2 and C_4 products, and developing strategies to further limit aldo-ketohexose interconversion to gain better control over the distribution of C_3 vs. C_2/C_4 products. The partially oxidized products may be formed by the reduction of Mo(VI) to Mo(V) and/or Mo(IV)

because particles of MoO_3 appear to progressively turn dark blue over the course of the reaction. In this regard, 1,2-CS catalysts that do not readily reduce in the presence of carbohydrates have the potential to result in higher ultimate lactate yields. Quantification of reaction intermediates and by-products under these relatively mild retro-aldol conditions and their dependence on 1,2-CS and 1,2-HS site distribution are some of our current focus.

The use of moderate temperatures (~100 °C) enables numerous desirable features for the production of lactic acid and alkyl lactate from hexoses such as lower process pressure and reduced catalyst deactivation due to product deposition on the catalysts. The minimal operating pressure for such reactions is autogenous, and is largely determined by the vapor pressure (P^{sat}) of the solvent. For instance, for methanol, P^{sat} = 3.5 bar at 100 °C and P^{sat} = 21.9 bar at 170 °C (31). We note that, in the case of reactions in ethanol at 100 °C, after ethyl lactate production from the initially added fructose stops, e.g., see data in *SI Appendix*, Fig. S18, ~20 h, the MoO_3/Sn-MFI catalyst combination is still active without regeneration by calcination or washing, as indicated by further production of ethyl lactate upon introduction of additional fructose to the reaction solution. In our hands, this is contrary to the coked state of Sn-Beta catalysts that requires catalyst calcination after high-temperature reactions (3).

Materials and Methods

Reagents and Catalysts. A full list of chemicals used in this study and their sources can be found in *SI Appendix*. The hydrothermal syntheses of Sn-MFI and Sn-Beta molecular sieves were performed according to previously published procedures that are described in detail in *SI Appendix*.

Reaction Analysis. Carbohydrate analysis and fractionation were performed via HPLC on an Agilent Hi-Plex Ca column with refractive index and evaporative light scattering detectors. Alkyl lactates were quantified by GC with a flame ionization detector (FID), and naphthalene as an internal standard. Additional side products were identified by GC coupled with MS. ^{1}H and ^{13}C liquid NMR spectrometry was used for product identification. Reactions were performed in thick-walled crimp-sealed glass reactors (VWR) that were heated in a temperature-controlled oil bath. Aliquots were extracted at desired times and analyzed by HPLC, GC, and/or NMR. Reported yields are on a carbon basis. Detailed descriptions of procedures followed during reaction testing and product identification can be found in *SI Appendix*.

ACKNOWLEDGMENTS. We thank Dr. Mona Shahgholi (Caltech) for use of GC-MS. This work was financially supported as part of the Catalysis Center for Energy Innovation, an Energy Frontier Research Center funded by the US Department of Energy, Office of Science, Office of Basic Energy Sciences under Award DE-SC0001004. M.O. acknowledges funding from the National Science Foundation Graduate Research Fellowship Program under Grant DGE-1144469.

1. Werpy T, Petersen G (2004) *Top Value Added Chemicals from Biomass: Volume I–Results of Screening for Potential Candidates from Sugars and Synthesis Gas* (Pacific Northwest National Laboratory, Richland, WA).
2. Dusselier M, Van Wouwe P, Dewaele A, Makshina E, Sels BF (2013) Lactic acid as a platform chemical in the biobased economy: The role of chemocatalysis. *Energy Environ Sci* 6(5):1415–1442.
3. Holm MS, Saravanamurugan S, Taarning E (2010) Conversion of sugars to lactic acid derivatives using heterogeneous zeotype catalysts. *Science* 328(5978):602–605.
4. Dusselier M, et al. (2013) Mechanistic insight into the conversion of tetrose sugars to novel α-hydroxy acid platform molecules. *ChemCatChem* 5(2):569–575.
5. Huber GW, Iborra S, Corma A (2006) Synthesis of transportation fuels from biomass: Chemistry, catalysts, and engineering. *Chem Rev* 106(9):4044–4098.
6. Dapsens PY, Mondelli C, Kusema BT, Verel R, Pérez-Ramírez J (2014) A continuous process for glyoxal valorisation using tailored Lewis-acid zeolite catalysts. *Green Chem* 16(3):1176–1186.
7. Dusselier M, Van Wouwe P, Dewaele A, Jacobs PA, Sels BF (2015) Shape-selective zeolite catalysis for bioplastics production. *Science* 349(6243):78–80.
8. Osmundsen CM, Holm MS, Dahl S, Taarning E (2012) Tin-containing silicates: Structure-activity relations. *Proc R Soc Lond A Math Phys Sci* 468(2143):2000–2016.
9. Tolborg S, et al. (2015) Tin-containing silicates: Alkali salts improve methyl lactate yield from sugars. *ChemSusChem* 8(4):613–617.
10. Gounder R, Davis ME (2013) Monosaccharide and disaccharide isomerization over Lewis acid sites in hydrophobic and hydrophilic molecular sieves. *J Catal* 308:176–188.
11. Bermejo-Deval R, Orazov M, Gounder R, Hwang S-J, Davis ME (2014) Active sites in Sn-Beta for glucose isomerization to fructose and epimerization to mannose. *ACS Catal* 4(7):2288–2297.
12. Bilik V, Petrus L, Farkas V (1975) Reactions of saccharides catalyzed by molybdate ions. XV. Mechanism of the epimerization reaction. *Chem Zvesti* 29(5):690–693.
13. Tanase T, et al. (1988) Novel C-2 epimerization of aldoses promoted by nickel(II) diamine complexes, involving a stereospecific pinacol-type 1,2-carbon shift. *Inorg Chem* 27(23):4085–4094.
14. Hricovíniová Z, Hricovíni M, Petrus L (1998) Stereospecific molybdic acid-catalyzed isomerization of D-fructose to branched-chain aldose. The synthesis of D-hamamelose. *Chem Pap* 52(5):692–698.
15. Hricovíniová Z, Lamba D, Hricovíni M (2005) Structure of 2-*C*-(hydroxymethyl)-D-ribose (hamamelose) in the solid-state analyzed by CP MAS NMR and X-ray crystallography. *Carbohydr Res* 340(3):455–458.
16. Yanagihara R, Osanai S, Yoshikawa S (1992) Novel branching of a ketose promoted by the nickel(II)-diamine complex. The isomerization of D-fructose into D-hamamelose. *Chem Lett* 1992(1):89–90.
17. Petruš L, Petrušová M, Hricovíniová Z (2001) The Bílik reaction. *Glycoscience: Epimerisation, Isomerisation and Rearrangement Reactions of Carbohydrates*, ed Stütz AE (Springer, Berlin), pp 15–41.
18. Matulova M, Bilik V (1990) Reactions of saccharides catalyzed by molybdate ions 95 XLIIL. NMR spectra of the 2-ketoses in molybdate complexes. *Chem Papers* 44(1):97–103.
19. Ju F, VanderVelde D, Nikolla E (2014) Molybdenum-based polyoxometalates as highly active and selective catalysts for the epimerization of aldoses. *ACS Catal* 4(5):1358–1364.
20. Stockman R, Dekoninck J, Sels BF, Jacobs PA (2005) The catalytic epimerization of sugars over immobilized heptamolybdate: Comparison of resins, layered double hydroxides and mesoporous silica as support. Nanoporous Materials IV: *Proceedings of the 4th* International Symposium on Nanoporous Materials, eds Jaroniec M, Sayari A (Elsevier, Amsterdam), pp 843–850.
21. Sauvage J-P, Verchère J-F, Chapelle S (1996) A multinuclear NMR spectroscopy study of the tungstate and molybdate complexes of D-fructose and L-sorbose. *Carbohydr Res* 286(6):67–76.
22. Bílik V (1972) Reactions of saccharides catalyzed by molybdate ions. II. Epimerization of D-glucose and D-mannose. *Chem Papers* 26(2):183–186.
23. Zhang J, et al. (2014) Kinetic study of retro-aldol condensation of glucose to glycolaldehyde with ammonium metatungstate as the catalyst. *AIChE J* 60(11):3804–3813.
24. Pescarmona PP, et al. (2010) Zeolite-catalysed conversion of C3 sugars to alkyl lactates. *Green Chem* 12(6):1083–1089.
25. Mal NK, Ramaswamy V, Rajamohanan PR, Ramaswamy V (1997) Sn-MFI molecular sieves: Synthesis methods, ^{29}Si liquid and solid MAS-NMR, ^{119}Sn static and MAS NMR studies. *Microporous Mater* 12(4-6):331–340.
26. Caldeira MM, Gil VMS (1986) Complexes of Mo(VI) with lactic, thiolactic and thiomalic acids studied by NMR spectroscopy. *Polyhedron* 5(1-2):381–385.
27. Moliner M, Román-Leshkov Y, Davis ME (2010) Tin-containing zeolites are highly active catalysts for the isomerization of glucose in water. *Proc Natl Acad Sci USA* 107(14):6164–6168.
28. Dapsens PY, Mondelli C, Pérez-Ramírez J (2013) Highly selective Lewis acid sites in desilicated MFI zeolites for dihydroxyacetone isomerization to lactic acid. *ChemSusChem* 6(5):831–839.
29. Hayashi Y, Sasaki Y (2005) Tin-catalyzed conversion of trioses to alkyl lactates in alcohol solution. *Chem Commun (Camb)* (21):2716–2718.
30. Gunther WR, et al. (2012) Sn-Beta zeolites with borate salts catalyse the epimerization of carbohydrates via an intramolecular carbon shift. *Nat Commun* 3:1109.
31. Goodwin RD (1987) Methanol thermodynamic properties from 176 to 673 K at pressures to 700 bar. *J Phys Chem Ref Data* 16(4):799–892.